Journal of Luminescence 131 (2011) 850–855

Contents lists available at ScienceDirect

Journal of Luminescence

journal homepage: www.elsevier.com/locate/jlumin

Eu^{3+} photoluminescence enhancement due to thermal energy transfer in Eu_2O_3-doped SiO_2–B_2O_3–PbO_2 glasses system

S.A. Lourenço [a,c,*], N.O. Dantas [b], E.O. Serqueira [b], W.E.F. Ayta [b], A.A. Andrade [c], M.C. Filadelpho [d], J.A. Sampaio [d], M.J.V. Bell [e], M.A. Pereira-da-Silva [f,g]

[a] Universidade Tecnológica Federal do Paraná, Campus Londrina, CEP 86036-370, Londrina, Paraná, Brazil
[b] Laboratório de Novos Materiais Isolantes e Semicondutores (LNMIS), Instituto de Física, Universidade Federal de Uberlândia, CP593, 38400-902, Uberlândia, Minas Gearis, Brazil
[c] Grupo de Propriedades Ópticas e Térmicas de Materiais (GPOTM), Instituto de Física, Universidade Federal de Uberlândia, CP593, 38400-902, Uberlândia, Minas Gearis, Brazil
[d] Laboratório de Ciências Físicas, Universidade Estadual do Norte Fluminense, CEP 28013-602, Campos dos Goytacazes, Rio de Janerio, Brazil
[e] Departamento de Física, Universidade Federal de Juiz de Fora, CEP 36036-330, Juiz de Fora, Minas Gearis, Brazil
[f] Instituto de Física de São Carlos USP, CEP 13560-250, São Carlos, SP, Brazil
[g] Centro Universitário Central Paulista, UNICEP, CEP 13563-470, São Carlos, São Paulo, Brazil

ARTICLE INFO

Article history:
Received 17 May 2010
Received in revised form
10 November 2010
Accepted 26 November 2010
Available online 2 December 2010

Keywords:
Eu^{3+}-doped glass
Nanocrystals
Lead borosilicate glasses
Optical properties
Photoluminescence
Energy transfer process

ABSTRACT

In this work, Eu^{3+}-doped lead borosilicate glasses (SiO_2–B_2O_3–PbO_2) synthesized by fusion method had their optical properties investigated as a function of temperature. Atomic Force Microscopy images obtained for a glass matrix annealed at 350 and 500 °C show a precipitated crystalline phase with sizes 11 and 21 nm, respectively. Besides, as the temperature increases from 350 to 300 K a strong Eu^{3+} photoluminescence (PL) enhancement takes place. This anomalous feature is attributed to the thermally activated carrier transfer process from nanocrystals and charged intrinsic defects states to Eu^{3+} energy levels. In addition, the PL peaks in this temperature range were assigned to the Eu^{3+} transitions $^5D_0 \rightarrow {}^7F_2$, at 612 nm, $^5D_0 \rightarrow {}^7F_1$, at 595 nm, and $^5D_0 \rightarrow {}^7F_0$, at 585 nm. It was also observed that the $^5D_0 \rightarrow {}^7F_3$ and $^5D_0 \rightarrow {}^7F_4$ PL bands at 655 and 700 nm, respectively, show a continuous decrease in intensity as the temperature increases.

1. Introduction

In the last decade great attention has been paid to trivalent lanthanide-doped materials due to their applicability as solid-state laser medium, fiber amplifiers, infrared-to-visible up-converters, phosphors, and field emission displays [1–4]. In this context, glasses are the most investigated host materials because of the relative ease of their fabrication, shaping, flexibility to add active ions in different concentrations, and the possibility of easily obtaining bulk samples when compared to single crystalline matrices.

Among several glass systems, oxide glasses are the most stable active ions host for practical applications such as optical and sensor devices, mainly due to their high chemical durability and thermal stability. Lead borosilicate glasses, for example, present low thermal expansion coefficient of about $3.4 \times 10^{-6}\ K^{-1}$ and low dielectric constant, characteristics that make them suitable for applications as low-dielectric ceramic substrates to be used at low temperatures [5,6].

In this paper, photoluminescence (PL) as a function of temperature and excitation intensity, as well as the optical absorption (OA) spectra were measured to investigate the optical properties of SBP (SiO_2–B_2O_3–PbO_2) Eu^{3+}-doped glasses system. An additional study was made, by measuring these properties of samples prepared in different conditions, i.e., as cast and annealed at two temperatures. The Atomic Force Microscopy (AFM) images are used to corroborate the PL results.

2. Samples and experimental details

The SBP glass samples were synthesized with nominal compositions $40SiO_2$:$40B_2O_3$:$20PbO_2$ (mol%) by adding xEu_2O_3 (wt%), with $x=2.0$. The powder mixtures were melted in an alumina crucible at 1300 °C for 30 min in air atmosphere. Afterwards, they were quenched to room temperature. Then, the obtained cooled glasses were thermally annealed at 350 °C for 24 h to reduce internal stresses. An additional set of samples were heat-treated at 500 °C for 120 h to induce crystallization process. Afterwards, these samples were cut into slabs of about 1.5 mm-thick and optically polished.

The optical absorption (OA) measurements were carried out at room temperature using a UV–vis–NIR Shimadzu UV-3600 spectrometer. The excitonic transitions were obtained by measuring the

* Corresponding author at: Universidade Tecnológica Federal do Paraná, Campus Londrina, CEP 86036-370, Londrina, Paraná, Brazil.
E-mail address: lourenco-sidney@hotmail.com (S.A. Lourenço).

0022-2313 © 2010 Elsevier B.V. Open access under the Elsevier OA license.
doi:10.1016/j.jlumin.2010.11.028

photoluminescence (PL) spectra recorded using a SPEX-750 M monochromator equipped with a Joban-Yvon CCD 2000 × 800-3, in the 30–300 K temperature range. The sample temperature variation was controlled using a closed-cycle He cryostat (Janis, model CCS-150) equipped with a LakeShore temperature controller (model 805). An argon ion laser focused on ~120 μm ray spot and operating at wavelength of 514.5 nm was used for excitation of the samples. The AFM images were obtained with a Multimode Nanoscope IIIa (Digital Instruments, Veeco).

3. Experimental results and discussion

Fig. 1(A) shows the optical absorption spectra of Eu^{3+} SBP glass samples. One can observe that the Eu^{3+} 4*f*–4*f* transitions originated from the ground state $^7F_0$. The peaks at 394 and 465 nm correspond to the $^7F_0 \rightarrow {}^5L_6$ and $^7F_0 \rightarrow {}^5D_2$ transitions, respectively.

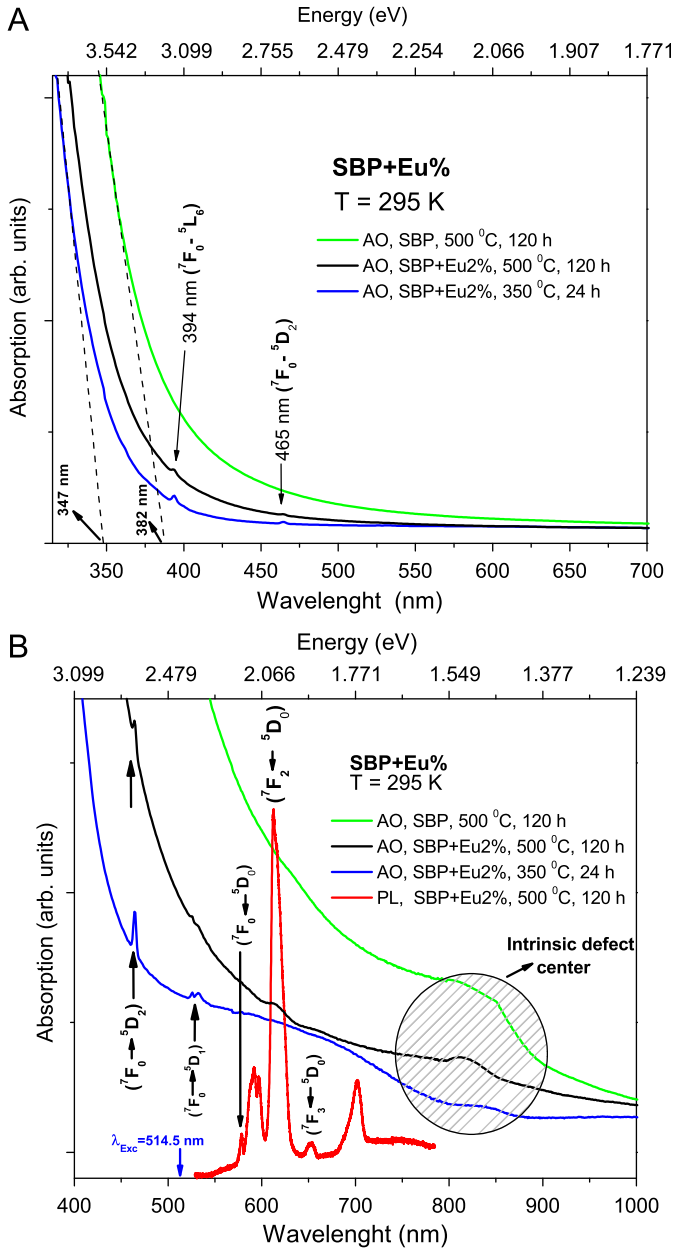

Fig. 1. (A) Optical absorption spectra of SBP samples containing Eu^{3+}. The thickness of the samples was approximately 1.5 mm. (B) Shows photoluminescence and optical absorption spectra obtained on the same samples.

The UV–vis spectra indicate that the SBP glass matrix has an optical band gap energy (E_{gap}) of 3.24 eV (382 nm) when annealed at 500 °C. By extrapolating the linear portion of the optical absorption curve or its tail, it is possible to verify that E_{gap} value increases to 3.38 eV (367 nm) as Eu^{3+} ions are incorporated in the SBP glass matrix. One can also note that the heat treatment at higher temperature induces a red shift of the electronic absorption edge towards larger wavelengths, which is in good agreement with results reported previously for TeO_2- [7] and SiO_2- [8] based glasses and it is related to glass crystallization process.

Fig. 1(B) depicts both absorption and luminescence spectra of Eu^{3+} SBP glasses in the 400–1000 nm spectral range. It can be noted that a series of Eu^{3+} characteristic emission lines between 540 and 780 nm, including the most prominent peak at 612 nm corresponds to the $^5D_0 \rightarrow {}^7F_J$ (J=0, 1, 2, 3, 4) transitions [9–11]. In addition, the optical absorption spectrum for the undoped and Eu-doped samples shows a weak shoulder at about 620 nm and another more intense one at 820 nm. In the case of Eu-doped SBP glass, as the heat treatment temperature increases the shoulder about 620 nm narrows, indicating that a nucleation process takes place. On the other hand, for the undoped sample, this shoulder is not so evident due to the E_{gap} red shift. This feature is assigned for nanocrystalization from glass matrix and intrinsic impurities presented in the raw precursors of the vitreous matrix [7,12–14].

The PL spectra of SBP matrix obtained at different temperatures are shown in Fig. 2. As can be seen, at low temperatures, an intense and asymmetric broad luminescence peak arises in the same spectral region of the Eu^{3+} transition, $^5D_0 \rightarrow {}^7F_4$. The intensity of this PL band is strongly temperature-dependent and falls by approximately 6.7 orders of magnitude between 35 and 300 K.

This broad luminescence band centered around 690 nm has also been reported in silicate [12], chalcogenide [13], tellurite (TeO_2-based) [7], and Er^{3+}-doped TeO_2 [14] glasses. The authors of these works claim that such a band is due to charged intrinsic defects in the glass network with deep energy levels, such as oxygen deficient centers in tellurite and silicate glasses or as dangling bonds in chalcogenide glasses. A broad visible PL band, with a large Stokes shift, has been also related to the recombination of self-trapped excitons in anatase TiO_2 nanocrystals dispersed in water solution [15]. Structural order–disorder in several ceramics prepared by the solid-state reaction method [16] and by the

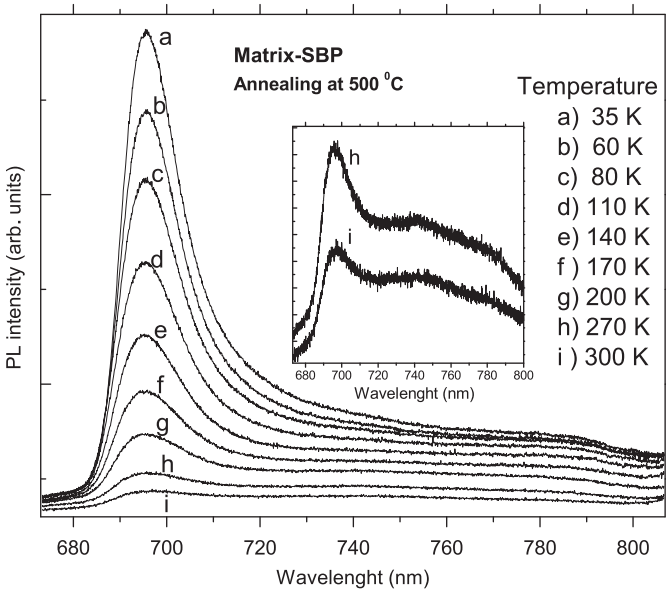

Fig. 2. Photoluminescence spectrum of SBP matrix annealed at 500 °C as a function of temperature. Excitation was performed at 514.5 nm using an Ar^+ laser.

polymeric precursor method [17,18] has been used to explain the room temperature PL spectra observed in these amorphized materials. Such studies have shown that the broad PL emission band, covering a large part of the visible spectra of the structurally disordered compounds, is very similar to that observed for nanocrystalline PL emission [15,18]. As can been seen, there is no general consensus in the current literature about the origin of luminescence at room temperature in amorphized structures.

Furthermore, the crystallization process is still a serious issue during the synthesis of borosilicate glass, and its trigger mechanism has been investigated by several researchers. For example, it was found that cristobalite could be formed in the synthesis process [19], and phase separation was the key step in this crystallization process. In fact, according to activation energy analysis [20] it was suggested that devitrification is controlled by the transport of alkali ions in borosilicate glass. Indeed, several crystalline oxides, such as Al_2O_3 [19,21], Ga_2O_3 [22], and mixed alkaline earth oxides [23], have been previously identified to inhibit cristobalite formation during firing of the borosilicate glass.

In order to clarify this question, AFM images of undoped SBP and Eu^{3+}-doped SBP samples, as shown in Fig. 3, became very useful. One can observe from AFM images the formation of nanocrystals (NCs) in a very definite shape. In the case of the undoped SBP sample heat treated at 350 °C for 24 h, it is possible to identify NCs

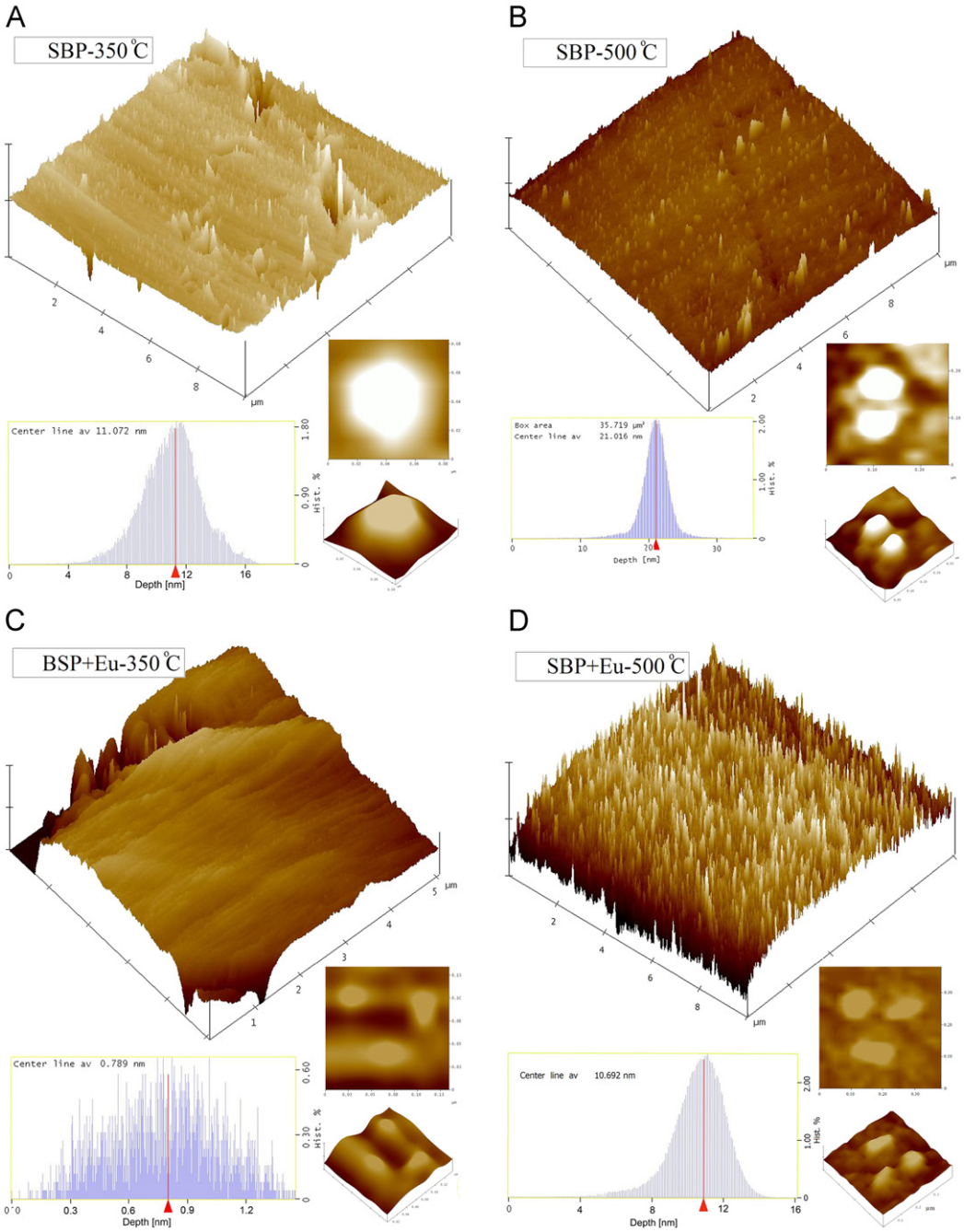

Fig. 3. Atomic force micrographs of SBP and Eu^{3+}-doped SBP glasses prepared by the fusion method. (A) and (B) show SBP glass annealed at 350 °C for 24 h and 500 °C for 120 h, respectively. (C) and (D) show Eu^{3+}-doped SBP glass annealed at 350 °C for 24 h and 500 °C for 120 h, respectively. In the right margin, the AFM morphology of isolated NCs is shown in two-dimensional (2D) and three-dimensional (3D) images. The average size estimated and their distributions are shown in the blue spectra. The average size is represented by red line. (For interpretation of the references to color in this figure legend, the reader is referred to the web version of this article.)

of about 11 nm. As heat treatment temperature/time increases, the size of such NCs grows to about 21 nm, which is a known result in the literature [24]. On the other hand, when 2% of Eu_2O_3 is added to the SBP matrix one can observe a very prominent decrease in the NCs size independently if the heat treatment is performed at 350 or 500 °C. Therefore, the AFM images indicate that nanocrystallization is inhibited by adding Eu_2O_3 into the SBP glass composition. In fact, Song et al. [25] analyzed the influence of dopants on the borosilicate glass crystallization and found that some network modifiers such as CeO_2 and La_2O_3 that are lanthanide oxides like Eu_2O_3, avoid cristobalite formation in borosilicate glasses.

Based on the above statements, the broad absorption and luminescence in the visible region can be associated to the formation of nanocrystallized glasses (probably cristobalite particles embedded in the glass matrix during firing of the borosilicate glass) and to intrinsic defects related to the glass matrix with deep energy levels. It is well-known that crystallization of glass systems is one of the effective methods for the fabrication of nanostructures [26]. In recent times, crystallized glasses consisting of nonlinear optical/ferroelectric nanocrystals, *i.e.*, nanocrystallized glasses, have received special attention because of its high potential for applications in the photonic area, such as tunable waveguide and optical switching devices [27]. Two kinds of transparent TeO_2-based nanocrystallized glasses have been developed: K_2O–Nb_2O_5–TeO_2 system, showing a second harmonic generation [28] and BaO–Ln_2O_3–TeO_2 (Ln: rare-earth) system, consisting of $Ln_2Te_6O_{15}$ or $Ln_2Te_5O_{13}$ nanocrystals, having an average grain size around 50–100 nm [26]. In addition, Narita et al. [29] investigated nanocrystalization of K_2O–Nb_2O_5–GeO_2 glass and observed the crystalline phase of KNbGeO, with crystal size around 10 nm. More recently, nanocrystalization of ferroelectric lithium niobate in $LiNbO_3$–SiO_2 glasses was observed by Prapitpongwanich et al. [30], whose average crystal size was about 13 nm. Besides, they claim that a decrease in the nanocrystal size can be achieved by annealing the samples at lower temperatures.

As can be seen in Fig. 2, the obtained PL emission band around 1.77 eV (700 nm) does not change with the temperature, from 35 up to 300 K, showing a high thermal stability for this optical transition. Indeed, this result is in agreement with the previously reported papers that state that highly located defect states and the formation of nanocrystallized glass can be related to the fact that nanocomposites in glasses and deeper energy levels of the defects show a low temperature dependence of the optical transition energy [31–33], in contrast to the strong temperature dependence of the optical gap observed for glasses [34,35].

In order to better clarify the nature of the strong emission band at the visible spectral region for temperatures near the room temperature and the nature of NCs, a detailed investigation considering additional optical measurements, heat treatment on samples, structural characterization, as well as new SBP samples with different Eu concentration is being taken into account and will be discussed in further works.

It is worthy of mentioning that charged intrinsic defects are known to create additional electric fields in the vicinity of the dopants [7,12–14]. In the case of SBP glasses, the electrons or holes initially trapped in these defect centers can easily get excited thermally. As the temperature increases, charger carriers with energy above $^5D_0$ state, are slowly thermally delivered, which in turn results in an additional radiative decay in the ^7F_J ($j=0,1,2,3,4$) energy levels. In fact, previous studies have indicated that photo-excited defect electrons migrated to the recombination sites traps [12]. If such an electron, located in the vicinity of a photo-excited Eu^{3+} migrates to another location, the electric field at the location of the Eu^{3+} ion changes. Besides, due to vibrational interaction of Eu atoms with the neighborhood, the intrinsic luminescence is largely Stokes shifted and broad [36]. According to experimental data, a simplified energy level scheme for the Eu^{3+} ions and the optical transitions observed in Figs. 1 and 2 are indicated in Fig. 4.

The photoluminescence spectra obtained at several temperatures in vitreous ceramic samples are shown in Fig. 5. One can note that as temperature increases, the intensity of luminescence band centered about 696 nm presents a fast decrease (thermal quenching), which is attributed to the thermal energy activation of the NCs states and charged intrinsic defects of the lead borosilicate glasses with subsequent non-radiative recombination (see Figs. 2 and 4). On the other hand, the intensity of luminescence band centered

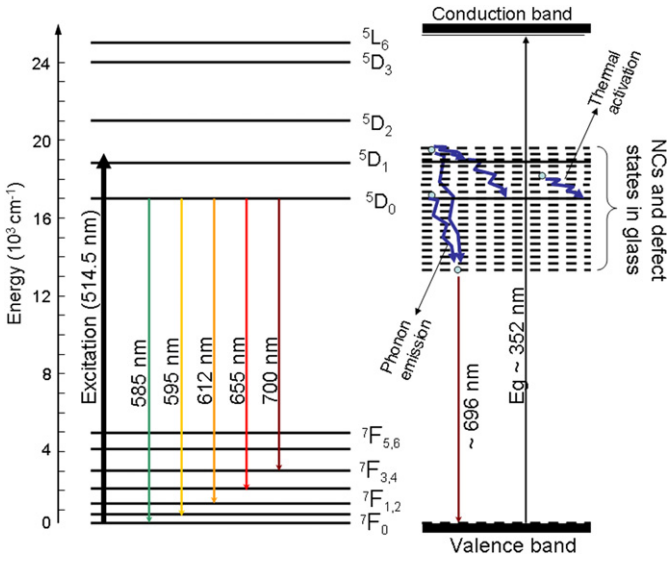

Fig. 4. Simplified energy levels scheme of Eu^{3+} ions with indication of the radiative transitions observed. The shaded lines indicate the approximated NCs and defect band location. To simplify, the energy level states between $^5D_1$ state and the glass matrix conduction band are not shown, as can be seen in optical absorption spectra in Fig. 1B.

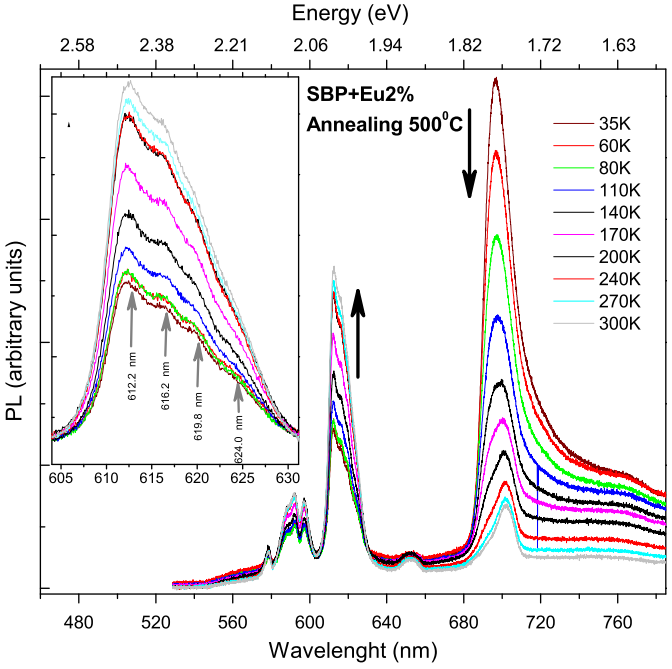

Fig. 5. Photoluminescence spectra of 2% Eu^{3+}-doped SiO_2–B_2O_3–PbO_2 glasses for different temperatures. Inset shows a large spectral range of principal Eu^{3+} luminescence band centered at 616.2 nm.

about 612 and ~595 nm, respectively, due to the ($^5D_0 \rightarrow {}^7F_2$) and ($^5D_0 \rightarrow {}^7F_1$) transitions shows a strong increase as the temperature increases. The thermal energy transfer between dots and ions may occur because special sizes of NCs emit photons in the energy range that overlaps the europium transitions.

The inset in Fig. 5 shows the $^5D_0 \rightarrow {}^7F_2$ recombination in a lower energy scale. For the $^5D_0 \rightarrow {}^7F_2$ transition it is possible to observe four broad overlapping lines in the region 605–630 nm, corresponding to emission of the four Stark components of the $^7F_2$ state [37]. So, the Stark splitting of the $^5D_0 \rightarrow {}^7F_{1,2}$ transitions reveals that the Eu^{3+} ions are in states of low symmetry, as expected for a glass matrix.

The temperature dependence of PL peak intensity for the bands centered at 612 and 696 nm obtained from samples annealed at 350 and 500 °C, respectively, shown in Fig. 6, presents two remarkable features. First, the peak intensity at 696 nm decreases quickly and does not depend on thermal annealing, and secondly the intensity of the peak centered at 612 nm ($^5D_0 \rightarrow {}^7F_2$ transition) presents a significant decrease in its value as temperature increases. This fact can be related to the crystallization process induced by nanocrystals with emission around the visible region that takes place when the samples are heat-treated, which suggests a change in the structural arrangement from the glassy to vitreous ceramic form, resulting in a decrease in the interatomic positions in order to occupy those sites with a lesser energy value. To verify the results of the fluorescence decay, the time-resolved photoluminescence spectra of the SBP annealed at 350 and 500 °C were measured with 532 nm excitation, as shown in Fig. 7. The decay curves of luminescence were fitted by a single-exponential function: $D(t)=c_0 \exp(-t/\tau)$, where c_0 is a constant, t is the time and τ is the relaxation time. The obtained lifetime of 1.93 ms for 2% Eu-doped glass annealed at 350 °C is shorter than the lifetime of the glass annealed at 500 °C, i.e. 1.96 ms. It is well-known that the intensity of the electric-dipole $^5D_0 \rightarrow {}^7F_2$ transition is significantly affected by the degree at the center of symmetry in the environments around Eu^{3+} ions, and that the intensity of an emission transition is proportional to the radiative decay of these transitions [38]. When Eu^{3+} ions are situated at low-symmetry sites, there is a high probability of the electric-dipole transition to occur [39,40]. Since the emission peak intensity around 612 nm, corresponding to the $^5D_0 \rightarrow {}^7F_2$ Eu^{3+} transition, obtained on a Eu-doped SBP sample annealed at 350 °C is more intense than that annealed at 500 °C, as observed in the Fig. 6, it is evident that the latter is situated at lower-symmetry sites. This result is consistent with the fact that crystallization of glass increases with the increase in heat-treatment temperature. As a matter of fact, Chen, et al. [41], observed that the heat treatment regime plays an important role in the lifetime of Eu^{3+} transitions $^5D_0 \rightarrow {}^7F_J$ ($J=0, 1, 2, 3, 4$) as Eu is added to $SiO_2-Al_2O_3-NaF-GdF_3$ glass system, agreeing with present results on Eu-doped SBP glasses.

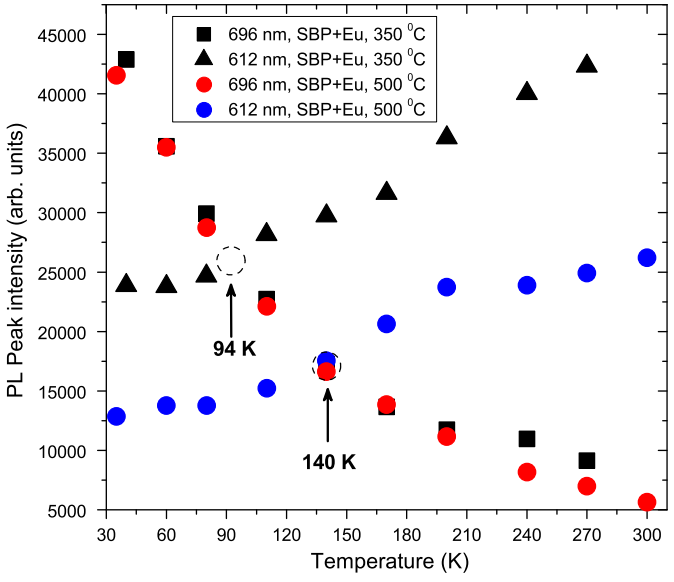

Fig. 6. Temperature dependence of PL peak intensity for the bands centered at 696 and 612 nm annealed at 350 and 500 °C. The shift to higher intensity of 612 nm emission band of sample annealed at low temperature (black triangle), in relation to one annealed at high temperature (blue circle), is due to glass crystallization effect (see discussion in the text for more details). (For interpretation of the references to color in this figure legend, the reader is referred to the web version of this article.)

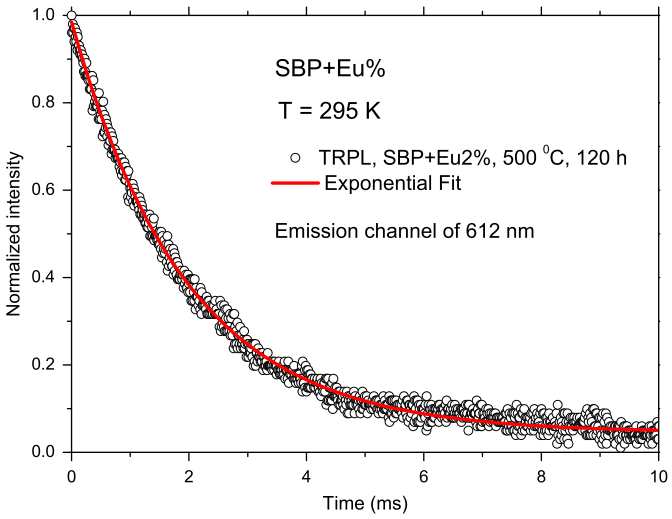

Fig. 7. Decay curve (open circle) and fitted curve (red line) of the luminescent excited state $^5D_0$ to $^7F_2$ for the SBP+Eu2% annealed at 500 °C for 120 h. The excitation was 532 nm with emission at 612 nm. The time resolution of the apparatus is 0.1 μs. (For interpretation of the references to color in this figure legend, the reader is referred to the web version of this article.)

4. Conclusions

In summary, the optical properties of Eu^{3+}-doped lead borosilicate glasses (SiO_2–B_2O_3–PbO_2), synthesized by the melt-quenching method, was analyzed using photoluminescence spectroscopy as a function of temperature (35 K ≤ T ≤ 300 K) as well as absorption spectroscopy at room temperature.

The origin of the broad absorption and luminescence in the visible region, in Eu^{3+}-doped lead borosilicate glasses, can be associated to the formation of nanocrystals (probably cristobalite) embedded in the glass matrix during firing of the borosilicate glass and to intrinsic defects related to the glass matrix with deep energy levels. AFM images show that spontaneous nanocrystallization occurs in the SBP glass matrix, presenting very definite crystal shapes. It was shown that by increasing heat treatment temperature/time or by adding Eu ions to the glass matrix, the nanocrystals size can be controlled.

An unusual PL intensity enhancement with temperature increase, obtained on Eu^{3+}-doped lead borosilicate glasses is observed. The anomalous temperature dependence of PL spectra indicates an efficient energy transfer mechanism from the NCs and the host defects to Eu^{3+} ions.

Finally, due to strong red luminescence of Eu^{3+}, Eu-doped lead borosilicate glass synthesized by melt-quenching methods, proves to be a good candidate to be used for manufacturing highly luminescent sealing glasses compatible with silicon photodetectors and solar cells.

Acknowledgments

The authors would like to acknowledge the financial support granted by the following Brazilian agencies: CAPES, MCT/CNPq and FAPEMIG.

References

[1] A. Biswas, G.S. Maciel, R. Kapoor, C.S. Friend, P.N. Prasad, Appl. Phys. Lett. 82 (2003) 2389.
[2] F. Roy, F. Leplingard, L. Lorcy, A. Le Sauze, P. Baniel, D. Bayart, Electron. Lett. 37 (2001) 943.
[3] J.L. Doualan, S. Girard, H. Haquin, J.L. Adam, J. Montagne, Opt. Mater. 24 (2003) 563.
[4] H. Lin, K. Liu, E.Y.B. Pun, T.C. Ma, X. Peng, Q.D. An, J.Y. Yu, S.B. Jiang, Chem. Phys. Lett. 398 (2004) 146.
[5] Jau-Ho Jean, Chia-Ruey Chang, Tong-Hua Kuan, C.H. Lin, Mater. Chem. Phys. 42 (1995) 5661 references therein.
[6] M.T. Sebastian, H. Jantunen, Int. Mater. Rev. 53 (2008) 57.
[7] V.K. Tikhomirov, S. Ronchin, M. Montagna, M. Ferrari, D. Furniss, Phys. Status Solidi (a) 187 (2001) R4.
[8] J. Fu, J.M. Parker, P.S. Flower, R.M. Brown, Mater. Res. Bull. 37 (1843) 2002.
[9] M. Peng, Z. Pei, G. Hong, Q. Su, J. Mater. Chem. 13 (2003) 1202.
[10] M. Pang, J. Lin, J. Fu, R. Xing, C. Luo, Y. Han, Opt. Mater. 23 (2003) 547.
[11] H. Meyssamy, K. Riwotzki, Adv. Mater. 11 (1999) 840.
[12] L.N. Skuja, J. Non-Cryst. Solids 239 (1998) 16.
[13] V.K. Tikhomirov, K. Lakoubovskii, P.W. Hertogen, G.J. Adriaenssens, Appl. Phys. Lett. 71 (1997) 2740.
[14] V.K. Tikhomirov, A.B. Seddon, D. Furniss, M. Ferrari, J. Non-Cryst. Solids 326 (2003) 296.
[15] L. Cavigli, F. Bogani, A. Vinattieri, V. Faso, G. Baldi, J. Appl. Phys. 106 (2009) 053516 references therein.
[16] T. Badapanda, S.K. Rout, L.S. Cavalcante, J.C. Sczancoski, S. Panigrahi, E. Longo, M.S. Li, J. Phys. D: Appl. Phys. 42 (2009) 175414.
[17] V.M. Longo, et al., J. Appl. Phys. 104 (2008) 023515;
E. Longo, et al., J. Phys. Chem. A 112 (2008) 8953;
F.M. Pontes, et al., J. Lumin. 104 (2003) 175.
[18] J. Milanez, A.T. Figueiredo, S.R. de Lazaro, V.M. Longo, R. Erlo, V.R. Mastelero, R.W.A. Franco, E. Longo, J.A. Varela, J. Appl. Phys. 106 (2009) 043526.
[19] J.-H. Jean, T.K. Gupta, J. Am. Ceram. Soc. 76 (2010) 1993.
[20] J.-H. Jean, T.K. Gupta, J. Mater. Res. 7 (1992) 3103.
[21] W.-F. Du, K. Kuraoka, T. Akai, T. Yazawa, J. Mater. Sci. 35 (2000) 4865.
[22] J.-H. Jean, T.K. Gupta, J. Mater. Res. 8 (1767) 1993.
[23] S. Liu, G. Zhao, H. Ying, J. Wang, G. Han, J. Non-Cryst. Solids 354 (2008) 956.
[24] R.S. Silva, P.C. Moraes, A.M.A. Milla, Qu Fanyao, A.F.G. Monte, N.O. Dantas, J. Non-Cryst. Solids 352 (2006) 3522.
[25] S. Song, Z. Wen, Yu Liu, Q. Zhang, X. Wu, J. Zhang, J. Han, Ceram. Int. 35 (2009) 3037.
[26] Y. Fujimoto, Y. Benino, T. Fujiwara, R. Sato, T. Komatsu, J. Ceram. Soc. Jpn. 109 (2001) 466.
[27] K. Naito, Y. Benino, T. Fujiwara, T. Komatsu, Solid State Commun. 131 (2004) 289.
[28] R. Sakai, Y. Benino, T. Fujiwara, R. Sato, T. Komatsu, Appl. Phys. Lett. 77 (2000) 2118.
[29] K. Narita, Y. Takahashi, Y. Benino, T. Fujiwara, T. Komatsu, J. Am. Ceram. Soc. 87 (2004) 113.
[30] P. Pratitpongwnich, R. Harizanova, K. Pengpat, C. Russel, Mater. Lett. 63 (2009) 1027.
[31] S.G. Lu, C.L. Mark, G.K.H. Pang, K.H. Wong, K.W. Cheah, Nanotechnology 19 (2008) 035702.
[32] N.O. Dantas, Q. Fanyao, A.F.G. Monte, R.S. Silva, P.C. Morais, J. Non-Cryst. Solids 352 (2006) 3525.
[33] A. Olkhovets, R.C. Hsu, A. Lipovskii, F.W. Wise, Phys. Rev. Lett. 81 (1998) 3539.
[34] J. Schwarz, H. Ticha, L. Tichy, Mater. Lett. 61 (2007) 520.
[35] J. Ozdanova, H. Ticha, L. Tichy, J. Non-Cryst. Solids 353 (2007) 2799.
[36] R.A. Street, Adv. Phys. 25 (1976) 397.
[37] S. Surendra Babu, P. Babu, C.K. Jayasankar, W. Sievers, Th. Troster, G. Wortmann, J. Lumin 126 (2007) 109.
[38] G. Lakshminarayana, S. Buddhudu, Mater. Chem. Phys. 102 (2007) 18.
[39] X. Fan, X. Wu, M. Wang, J. Qiu, Y. Kawamoto, Mater. Lett. 58 (2004) 2217.
[40] J. Wang, H. Song, X. Kong, H. Peng, B. Sun, B. Chen, J. Zhang, W. Xu, H. Xia, J. Appl. Phys. 93 (2003) 1482.
[41] Daqin Chen, Yuansheng Wang, Yunlong Yu, Ping Huang, J. Phys. Chem. C 112 (2008) 18943.